

Enrique Ruiz Arriola · Wojciech Broniowski

Proton-Proton On Shell Optical Potential at High Energies and the Hollowness Effect

October 9, 2018

Abstract We analyze the usefulness of the optical potential as suggested by the double spectral Mandelstam representation at very high energies, such as in the proton-proton scattering at ISR and the LHC. Its particular meaning regarding the interpretation of the scattering data up to the maximum available measured energies is discussed. Our analysis reconstructs 3D dynamics from the effective transverse 2D impact parameter representation and suggests that besides the onset of gray nucleons at the LHC there appears an inelasticity depletion (hollowness) which precludes convolution models at the attometer scale.

1 Introduction

The history of proton-proton scattering at high energies has been marked by continuous surprises; extrapolations have often been contradicted by actual measurements such as at ISR (see, e.g., [1; 2; 3; 4] for comprehensive accounts and references therein). The first run of the CERN-LHC on pp collisions has unveiled new features at CM energies about 7 TeV, measured by the TOTEM collaboration [5]. Contrary to naive expectations, probing strong interactions at such high energies, corresponding to a de Broglie wavelength of about half an attometer, becomes more intricate and may still be far from the asymptotics [6]. Regge phenomenology [7] motivated Barger and Phillips [8] to propose a parameterization which, when suitably extended, describes all ISR and the LHC data simultaneously [9; 10]. Dynamical calculations display the intricacy of non-perturbative phenomena at these high energies from a fundamental viewpoint (see e.g. [11; 12]). In the present talk we return to a phenomenological level and unveil interesting features of pp scattering via the so-called *on-shell optical potential model*.

The optical potential was first suggested to deal with inelastic neutron-nucleus scattering above the compound nucleus regime [13]. There, the concept of the black disk limit was first proposed and tested along with the observed Fraunhofer diffraction pattern [14], which also applies to the eikonal approximation [15]. The Serber model [16] was an incipient extension of the optical eikonal formalism to high energy particle physics. Based on a double spectral representation of the Mandelstam representation of the scattering amplitude, Cornwall and Ruderman delineated a definition of the optical potential directly rooted in field theory [17]. Field-theoretic discussions using the multichannel Bethe-Salpeter equation shed some further light

Talk presented by ERA at the Light Cone 2015 Conference, Frascati, Italy. 21-25 September 2015.

Supported by Spanish DGI and Feder funds (grant FIS2014-59386-P), by Junta de Andalucía (grant FQM225), and by Polish National Science Center (grant DEC-2012/06/A/ST2/00390).

Enrique Ruiz Arriola
Departamento de Física Atómica, Molecular y Nuclear and
Instituto Carlos I de Física Teórica y Computacional, Universidad de Granada, E-18071 Granada, Spain

Wojciech Broniowski
The H. Niewodniczański Institute of Nuclear Physics, Polish Academy of Sciences, PL-31342 Kraków, Poland, and
Jan Kochanowski University, PL-25406 Kielce, Poland
E-mail: Wojciech.Broniowski@ifj.edu.pl

[18; 19] (see, e.g., an early review on optical models [20]). The off-shell vs on-shell interplay was analyzed and an on-shell-type equation was proposed by Namyslowski [21]. The high energy grayness of the nucleon has been a matter of discussion since the 70's [22].

2 Amplitudes and parameterizations

The invariant proton-proton elastic scattering differential cross section is given by

$$\frac{d\sigma_{\text{el}}}{dt} = \frac{\pi}{p^2} \frac{d\sigma_{\text{el}}}{d\Omega} = \frac{\pi}{p^2} |f(s, t)|^2, \quad (1)$$

where $f(s, t)$ is the scattering amplitude having both the partial wave and the impact parameter expansions [23]

$$f(s, t) = \sum_{l=0}^{\infty} (2l+1) f_l(p) P_l(\cos \theta) = \frac{p^2}{\pi} \int d^2b h(\mathbf{b}, s) e^{i\mathbf{q}\cdot\mathbf{b}} = 2p^2 \int_0^{\infty} b db J_0(bq) h(b, s), \quad (2)$$

where $s = 4(p^2 + M^2)$, p is the CM momentum, and $t = -\mathbf{q}^2$ with $q = 2p \sin(\theta/2)$ denoting the momentum transfer. In the eikonal approximation one has $bp = l + 1/2 + \mathcal{O}(s^{-1})$, hence $h(b, s) = f_l(p) + \mathcal{O}(s^{-1})$ and $P_l(\cos \theta) \rightarrow J_0(qb)$. The total, elastic, and total inelastic cross sections read, respectively [23]

$$\sigma_T = \frac{4\pi}{p} \text{Im} f(\theta = 0) = 4p \int d^2b \text{Im} h(\mathbf{b}, s), \quad (3)$$

$$\sigma_{\text{el}} = \int d\Omega |f(s, t)|^2 = 4p^2 \int d^2b |h(\mathbf{b}, s)|^2, \quad (4)$$

$$\sigma_{\text{in}} \equiv \sigma_T - \sigma_{\text{el}} = \int d^2b n_{\text{in}}(b). \quad (5)$$

Here, the transverse probability inelastic profile fulfills $n_{\text{in}}(b) \leq 1$ and is given by

$$n_{\text{in}}(b) = 4p [\text{Im} h(b, s) - p |h(b, s)|^2]. \quad (6)$$

For our purposes we just need a working parameterization of the scattering amplitude. Here, and for definiteness we use the work in Ref. [9], and more specifically, their MBP2 form, which have been fitted separately for all known differential cross sections for $\sqrt{s} = 23.4, 30.5, 44.6, 52.8, 62.0,$ and 7000 GeV^1 and read

$$f(s, t) = \sum_n c_n F_n(t) s^{\alpha_n(t)}, \quad (7)$$

where $F_n(t)$ are form factors, $\alpha_n(t) = \alpha_n(0) + \alpha'_n(0)t$ and c_n are complex numbers which at variance with Regge theory [7], are assumed to be energy dependent. The fits produce $\chi^2/\text{d.o.f.} \sim 1.2 - 1.7$ [9; 10].

3 The on-shell optical potential

A general field theoretic approach requires solving a coupled channel Bethe-Salpeter equation involving all open channels, a most impractical a procedure, since their number becomes huge for the large energies at ISR or the LHC. Of course, a viable approach would be to determine the kernel, operating as a phenomenological optical potential, from the available NN scattering data. In the geometric picture, the diffraction pattern is manifest as a shadow of the inelastic scattering, such that the diffraction peak in the forward direction is due to a coherent interference. From a Quantum Mechanics point of view, the inelastic process can be interpreted as a leakage in the probability current. We propose a scheme below where a local and energy dependent potential can be directly computed from the data, unveiling the structure of the *inelasticity hole*.

A standard tool for handling the two-body relativistic scattering is the Bethe-Salpeter equation (we use conventions of Ref. [24]), which in the operator form reads

$$T = V + V G_0 T. \quad (8)$$

¹ A compilation of high energy scattering data can be found at <http://www.theo.phys.ulg.ac.be/alldata-v2.zip>.

For the $2 \rightarrow 2$ sector with the kinematics $(P/2 + k, P/2 - k) \rightarrow (P/2 + p, P/2 - p)$ it can be written as

$$T_P(p, k) = V_P(p, k) + i \int \frac{d^4 q}{(2\pi)^4} T_P(q, k) S(q_+) S(q_-) V_P(p, q), \quad (9)$$

where $q_{\pm} = (P/2 \pm q)$, P is the total momentum, $T_P(p, k)$ is the total scattering amplitude, and $S(q_{\pm})$ denotes the nucleon propagator. The kernel V represents the irreducible four-point Green's function, and it is generically referred to as the *potential*. Equation (9) is a linear four-dimensional equation. It requires the off-shell behavior of the potential $V_P(k', k)$ and generally depends on the choice of the interpolating fields, although one expects the scattering amplitude for the on-shell particles to be independent of the field choice.²

An approach which is manifestly independent of the off-shell ambiguities deduces an on-shell equation by separating explicitly those states which are on-shell and elastic from the rest [21] (for a similar and related ideas see, e.g., Ref. [24]). In the operator form, the final result can be written as (see also Ref. [17])

$$T_{\text{el}} = W + T_{\text{el}} G_0 T_{\text{el}}^{\dagger}, \quad (10)$$

where W is the *on-shell optical potential* and T_{el} is the elastic on-shell scattering amplitude,

$$T_{P,\text{el}}(p, k) = T_P(p, k)|_{p^2=k^2=s/4-M^2} = -8\pi\sqrt{s}f(s, t). \quad (11)$$

When written out explicitly, the equation becomes

$$T_{P,\text{el}}(p, k) = W_P(p, k) + i \int \frac{d^4 q}{(2\pi)^4} T_{P,\text{el}}(q, k) S(q_+) S(q_-) T_{P,\text{el}}(q, p)^*. \quad (12)$$

At the level of partial waves, we have a simplified form, which using $p(s) = (s/4 - M_N^2)^{\frac{1}{2}}$ reads

$$f_l(s) = w_l(s) + \frac{1}{\pi} \int_{s_0}^{\infty} ds' \frac{f_l(s') p(s') f_l(s')^{\dagger}}{s' - s - i0^+}, \quad (13)$$

where $s_0 = 4M_N^2$. Note that only the on-shell amplitude enters here, whereas the equation is non-linear. As usual, the scattering amplitudes are defined as boundary values of analytic complex functions, such that $f_l(s) \equiv f_l(s + i0^+)$. Note that due to the Schwartz reflection principle $f_l(s)^{\dagger} \equiv f_l(s - i0^+)$, and thus the unitarity condition corresponds to a right-hand discontinuity cut $2i\text{Im}f_l(s) = f_l(s + i0^+) - f_l(s - i0^+)$, which reads $\text{Im}f_l(s) - p(s)|f_l(s)|^2 = \text{Im}w_l(s)$ at $s > 4M_N^2$ and yields two contributions. The exchange, written as a left cut condition becomes $\text{Im}f_l(s) = \text{Im}w_l(s)$ for $s < 0$, whereas the causality implies a dispersion relation in energy along the left and right cuts. Invoking the eikonal approximation, which works phenomenologically for $\sqrt{s} \geq 23.5\text{GeV}$, and using Eq. (5) we get

$$w_l(s)|_{l+1/2=bp} = n_{\text{in}}(b)/4p + \mathcal{O}(s^{-1}) \quad (14)$$

Solving the BS equation becomes very complicated and for a phenomenological kernel is not truly essential. Instead, we use a *minimal relativistic approach* [25] based on the squared mass operator [26] defined as $\mathcal{M}^2 = P^{\mu} P_{\mu} + \mathcal{V}$, where \mathcal{V} represents the (invariant) interaction determined in the CM frame by matching to the non-relativistic limit with a local and energy-dependent phenomenological optical potential, $V(\mathbf{r}, s) = \text{Re}V(\mathbf{r}, s) + i\text{Im}V(\mathbf{r}, s)$. This yields $\mathcal{V} = 8M_N V(\mathbf{r}, s)$; it could be obtained by fitting elastic scattering data [25]. After quantization we have $\hat{\mathcal{M}}^2 = 4(\hat{p}^2 + M_N^2) + 8M_N V$, with $\hat{p} = -i\nabla$, such that the relativistic equation can be written as $\hat{\mathcal{M}}^2 \Psi = 4(k^2 + M_N^2) \Psi$, i.e., as a non-relativistic Schrödinger equation

$$(-\nabla^2 + M_N V) \Psi = (s/4 - M_N^2) \Psi. \quad (15)$$

This equation incorporates the necessary physical ingredients which were also present in the BS equation: relativity and inelasticity. The optical potential V *does not* yet correspond to the on-shell one defined by Eq. (10). The argument given in Ref. [17] uses the optical theorem from the continuity equation, yielding

$$\sigma_T - \sigma_{\text{el}} \equiv \sigma_{\text{in}} = -\frac{M_N}{p} \int d^3 x \text{Im} W(\mathbf{x}, s), \quad (16)$$

² This point is not made very clear in the literature; see, e.g., Ref. [24] for an explicit demonstration in the particular case of $\pi\pi$ scattering that the field transformations preserving the on-shell potential modify the on-shell T-matrix.

where the on-shell optical potential is defined by its imaginary part $\text{Im} W(\mathbf{x}, s) \equiv \text{Im} V(\mathbf{x}, s) |\Psi(\mathbf{x})|^2$ and can be interpreted as the local density of inelasticity at a given CM energy \sqrt{s} ; it also becomes $W = V + \dots$ perturbatively. Using $\sum_{l=0}^{\infty} (2l+1) [j_l(pr)]^2 = 1$, Eq. (16) becomes consistent with Eq. (14). We may further rewrite this in the impact parameter space by taking $\mathbf{x} = (\mathbf{b}, z)$ and integrating over the longitudinal component. As a result we get Eq. (5), where the transverse probability profile function is given by

$$n_{\text{in}}(b) = -\frac{M_N}{p} \int_{-\infty}^{\infty} dz \text{Im} W(\mathbf{x}, s) = -\frac{M_N}{p} \int_b^{\infty} \frac{2rdr}{\sqrt{r^2 - b^2}} \text{Im} W(r, s). \quad (17)$$

In last step the spherical symmetry has been exploited. To determine $W(r, s)$ we recognize this formula as an integral equation of the Abel type, hence it can be inverted using the standard method (see e.g. Ref. [27]) to give the on-shell optical potential *directly* from the inelasticity profile and hence from data,

$$\text{Im} W(r, s) = \frac{2p}{\pi M_N} \int_r^{\infty} db \frac{n'_{\text{in}}(b)}{\sqrt{b^2 - r^2}}. \quad (18)$$

This new formula is remarkable as it reconstructs the 3D on-shell dynamics from the effective transverse 2D impact parameter representation where the longitudinal physics has been integrated out.

4 Numerical results and discussion

For the MBP2 parameterization of Ref. [9] we obtain the inelastic profile function and its derivative for the measured and fitted energies $\sqrt{s} = 23.4, 30.5, 44.6, 52.8, 62.0$, and 7000 GeV. The result for 14000 GeV is an extrapolation proposed in Ref. [9]. The amplitudes of the on-shell potentials depend strongly on the CM energy \sqrt{s} , with a power-like behavior. Thus, in Fig. 1 we show the ratio normalized to the value at the origin, $\text{Im} W(r, s) / \text{Im} W(0, s)$. As can be vividly seen, the lower energy values have a maximum at the origin, whereas the LHC pp data develop a dip in the origin, which suggests that the inelasticity becomes maximal at a finite value, around $r = 1\text{fm}$. The fact that the optical potential has its maximum away from the origin is most remarkable; a feature shared by the profile function $n_{\text{in}}(b)$, which shows that in an inelastic collision most damage is not necessarily produced by central collisions. The ‘‘hollowness’’ effect is less evident in 2D as the 3D hole is integrated over the longitudinal variables which effectively fill the 3D-hole. This goes beyond the idea that the protons become ‘‘gray’’ above 13TeV, as recently suggested by Dremin [28] (see also [29; 30]), rather than a black disk. Actually, this shows in particular that the hollowness effect cannot be reproduced by an intuitive folding structure. Indeed, for small r we get

$$W(r) = \int d^3y \rho(\mathbf{y} + \mathbf{r}/2) \rho(\mathbf{y} - \mathbf{r}/2) = \int d^3y \rho(\mathbf{y})^2 - \frac{1}{4} \int d^3y [\mathbf{r} \cdot \nabla \rho(\mathbf{y})]^2 + \dots \quad (19)$$

showing that $W(0)$ is a local maximum, in contrast to the phenomenological result, see Fig. 1. This conclusion also holds if the folding is made between wave functions with no extra weight. Finally, we note that the mean squared radius of $\text{Im} W(r)$; $\langle r^2 \rangle = \frac{3}{2} \langle b^2 \rangle$ displays a logarithmic growth with the energy. These surprising new high energy features as well as the fluctuations in $n_{\text{in}}(b)$ [31] become relevant in heavy ions collisions and will be addressed in more detail elsewhere. The energy interpolation of [9] suggests that the 3D depletion already happens at 0.5 – 1TeV, below LHC energies, generating a flattening of the 2D impact parameter dependence.

5 Conclusions

The on-shell optical potential is a meaningful concept under the most common and general assumption of the Mandelstam double spectral representation. We have shown that it is also a useful quantity when interpreting the proton-proton scattering data at very high energies; the shape of the inelasticity hole changes dramatically when going from ISR to the LHC. The shoulder-like form of the imaginary part of the on-shell potential resembles very much the traditional pattern found in the absorptive part of optical potential in the neutron-nucleus reactions beyond the compound model regime [32]. For a heavy nucleus, the surface is much smaller than the volume and the shoulder merely shows that most inelastic processes occur at the surface. This can pictorially be imagined as derivatives of a Fermi-type distribution. In the case of the proton-proton scattering, extremely high energies seem necessary to resolve between the surface from the volume effects at the attometer scales. The puzzling hollowness effect sets in at 0.5 – 1TeV and awaits a dynamical explanation.

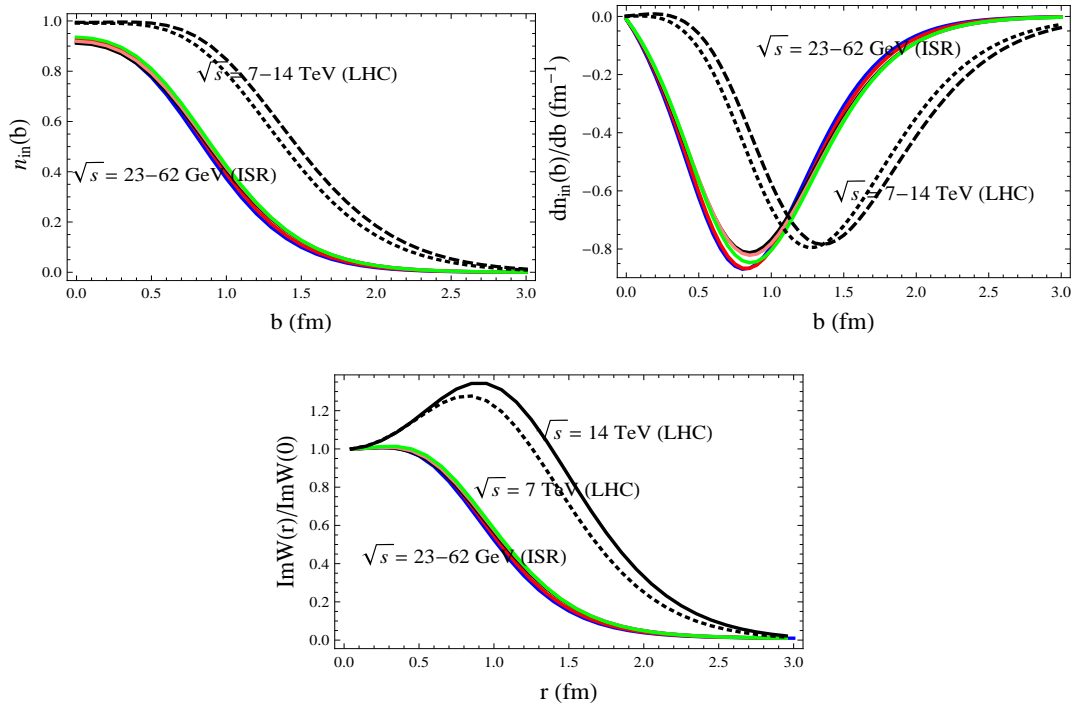


Fig. 1 Inelasticity properties of the proton-proton scattering at the CM energies $\sqrt{s} = 23.4, 30.5, 44.6, 52.8, 62.0, 7000,$ and 14000 GeV. Top: The inelastic profile (left) and its derivative (right) as a function of the impact parameter. Bottom: The imaginary part of the on-shell optical potential normalized to the value at the origin, plotted as a function of the radial distance.

References

1. U. Amaldi and Klaus R. Schubert. *Nucl.Phys.*, B166:301, 1980.
2. Hung Cheng and Tai Tsun Wu. *Expanding protons: Scattering at high energies*. Mit Pr, 1987.
3. G. Matthiae. *Rept. Prog. Phys.*, 57:743–790, 1994.
4. Vincenzo Barone and Enrico Predazzi. *High-Energy Particle Diffraction*. Springer-Verlag, Berlin Heidelberg, 2002.
5. G. Antchev et al. *Europhys. Lett.*, 101:21002, 2013.
6. D. A. Fagundes, M. J. Menon, and P. V. R. G. Silva. *Nucl. Phys.*, A946:194–226, 2016.
7. P. D. B. Collins, *An Introduction to Regge Theory and High-Energy Physics* Cambridge University Press 1977
8. R.J.N. Phillips and Vernon D. Barger. *Phys.Lett.*, B46:412–414, 1973.
9. D. A. Fagundes, A. Grau, S. Pacetti, G. Pancheri, and Y. N. Srivastava. *Phys.Rev.*, D88(9):094019, 2013.
10. O. V. Selyugin. *Phys. Rev.*, D91(11):113003, 2015. [Erratum: *Phys. Rev.D*92,no.9,099901(2015)].
11. V. A. Khoze, A. D. Martin and M. G. Ryskin, *Int. J. Mod. Phys. A* **30**, no. 08, 1542004 (2015)
12. E. Gotsman, E. Levin and U. Maor, *Int. J. Mod. Phys. A* **30**, no. 08, 1542005 (2015)
13. S. Fernbach, R. Serber, and T.B. Taylor. *Phys.Rev.*, 75:1352–1355, 1949.
14. J. Blatt and V. Weisskopf. *Theoretical nuclear physics*. Springer Science & Business Media, 2012.
15. RJ Glauber. *High energy collision theory*, volume 1 in *Lectures in theoretical physics*. Interscience, NewYork, 1959.
16. Robert Serber. *Reviews of Modern Physics*, 36(2):649, 1964.
17. John M Cornwall and Malvin A Ruderman. *Physical Review*, 128(3):1474, 1962.
18. Ronald Torgerson. *Physical Review*, 143(4):1194, 1966.
19. Richard C Arnold. *Physical Review*, 153(5):1523, 1967.
20. Muhammad M Islam. *Physics Today*, 25:23, 1972.
21. JM Namyslowski. *Physical Review*, 160(5):1522, 1967.
22. A. B. Kaidalov, *Phys. Rept.* **50**, 157 (1979).
23. R. Blankenbecler and M.L. Goldberger. *Phys.Rev.*, 126:766–786, 1962.
24. Juan Nieves and Enrique Ruiz Arriola. *Nucl. Phys.*, A679:57–117, 2000.
25. Enrique Ruiz Arriola and Wojciech Broniowski. *J. Phys. Conf. Ser.*, 630(1):012060, 2015.
26. T. W. Allen, G. L. Payne, and Wayne N. Polyzou. *Phys. Rev.*, C62:054002, 2000.
27. U Buck. *Reviews of Modern Physics*, 46(2):369, 1974.
28. I. M. Dremin. *arXiv:1511.03212*, hep-hp, 2015.
29. I. M. Dremin. *Phys. Usp.*, 56:3–28, 2013. [*Usp. Fiz. Nauk*183,3(2013)].
30. S. M. Troshin and N. E. Tyurin, *arXiv:1601.00483* [hep-ph].
31. Maciej Ryczyński and Zbigniew Włodarczyk. *J. Phys.*, G41:015106, 2013.
32. Peter Edward Hodgson. *Nuclear reactions and nuclear structure*. Clarendon Press, 1971.